Korean J. Chem. Eng., 32(8), 1688-1693 (2015)
DOI: 10.1007/s11814-014-0368-9

pISSN: 0256-1115
eISSN: 1975-7220

Properties of chitosan/magnetite nanoparticles composites for efficient dye adsorption and antibacterial agent

Yuvaraj Haldorai*,, Dian Kharismadewi*, Dirk Tuma***, and Jae-Jin Shim*,†**

*School of Chemical Engineering, Yeungnam University, Gyeongsan, Gyeongbuk 712-749, Korea
**Department of Energy and Materials Engineering, Dongguk University, Seoul 100-715, Korea
***BAM Federal Institute for Materials Research and Testing, Richard-Willstätter-Str. 11, D-12489 Berlin, Germany
(*Received 1 July 2014 • accepted 8 December 2014*)

Abstract−Chitosan (CS)/iron oxide (Fe_3O_4) composites were prepared using a chemical precipitation method. The CS/Fe_3O_4 composite was characterized by Fourier-transform infrared spectroscopy, X-ray diffraction, transmission electron microscopy, and zeta-potential measurements. The composite was used to remove methyl orange (MO) dye from an aqueous solution. The factors affecting the adsorption capacity, such as adsorption time, absorbent dosage and solution pH were investigated. The results suggested that the composite was an effective adsorbent for the removal of MO dye from its aqueous solution. Kinetics studies showed that the adsorption process was consistent with a pseudo-second-order model. The adsorbent efficiency was unaltered, even after five cycles of reuse, and the adsorbent could be recollected easily using a magnet. In addition, the composite exhibited a superior antibacterial efficacy against *Escherichia coli*; 82% within 24 h, as measured by the colony forming units.

Keywords: Chitosan, Fe_3O_4, Composite, Adsorbent, Antibacterial Agent

INTRODUCTION

The rapid industrialization over the past few decades has posed a major threat to the environment due to synthetic dyes in industrial effluents. Approximately 10-15% of the dyes are released as waste into the environment after their use in dyeing units [1]. Because the dyes are stable, recalcitrant, colorant, and even potentially carcinogenic and toxic, their release into the environment poses serious environmental, esthetic and health threats. Therefore, their removal from industrial effluents is a major environmental issue [2-4]. Among the physical, chemical and biological conventional methods of dye removal, physical adsorption is considered an effective method for the rapid removal of dyes from effluents [5]. Many adsorbents are available, including activated carbon [6], peat [7], silica [8], and clay [9]. Yet, despite these absorbents, the development of a more effective and cheaper adsorbent with a higher adsorption capacity and recycling ability would be desirable.

In this regard, chitosan (CS) is the most abundant natural polysaccharide after cellulose and hemicelluloses. Chitosan, a linear cationic, pH sensitive, non-toxic, biodegradable, and biocompatible polysaccharide obtained from the deacetylation of chitin appears to offer many distinct advantages [10,11]. CS is a super high-capacity adsorbent for the removal of contaminants in water with an adsorption capacity of 1,000-1,100 g/Kg, which is higher than that of activated carbon [12]. This high adsorption of CS is due to the abundance of hydroxyl and amino groups that can bind with contaminants. Due to the presence of large amounts of hydrogen bonding within CS, the adsorption capacity becomes smaller. Furthermore, the regeneration of CS by acid or base is simple and cost effective, but the application of acid or base for CS regeneration is not technically advantageous. The large amount of waste-water generated from the regeneration process requires further treatment, making the process non-environmentally friendly and unsustainable [13]. Therefore, metal oxides immobilized in a CS composite is a suitable candidate for the dye removal.

Metal oxides can be applied to a range of water-treatment processes owing to their high surface area as well as their low production and regeneration costs. Among the large family of metal oxides, magnetic nanoparticles have attracted considerable attention for their wide range of applications, such as medical diagnostics and therapeutics [14,15], magnetic resonance imaging (MRI) [16], catalysis [17], data storage [15], and environmental remediation [18]. Magnetic nanoparticles have been found to be chemically and biologically inert; they can be coated with polymers, enzymes, or antibodies to increase their functionalities for a range of applications. When the composite material is magnetic, it can be separated and recovered from the solution easily by the application of an external magnetic field, which opens a new door for easy and cost effective recovery of such adsorbents in water treatment.

Various research groups have reported the preparation of CS/Fe_3O_4 composites for different applications [19,20]. Zhu et al. [21] synthesized novel magnetic chitosan/poly(vinyl alcohol) hydrogel beads for dye removal. Liu et al. [22] fabricated magnetic cellulose-chitosan hydrogels from ionic liquids for the removal of heavy metal ions. Dodi et al. [23] prepared chitosan/iron oxide composite for Cu(II) removal. Wang et al. [24], Huang et al. [25], and Tran et al. [26] also reported the removal of Cu(II), Cr(VI), Pb(II), and Ni(II) using chitosan/magnetite composites. In this study, a CS/Fe_3O_4 com-

†To whom correspondence should be addressed.
E-mail: jjshim@yu.ac.kr

posite was designed to meet the needs of high adsorption, self-regeneration, easy separation, and cost-effective water treatment with enhanced antimicrobial properties. The immobilization of Fe_3O_4 onto the CS resolves the recollection and reuses limitation of CS. The CS/Fe_3O_4 composite was prepared using a chemical precipitation method and characterized by Fourier-transform infrared spectroscopy (FT-IR), X-ray diffraction (XRD), zeta-potential measurements, and transmission electron microscopy (TEM). The use of composite as a reusable adsorbent was examined through the effect of different parameters, such as the adsorbent dose, pH, reaction time, and recyclability.

EXPERIMENTAL

1. Materials

Chitosan (CS) with an 85% degree of deacetylation and molecular weight of 2.6×10^5 was purchased from Sigma-Aldrich. Ferric chloride hexahydrate ($FeCl_3\cdot6H_2O$), ferrous chloride tetrahydrate ($FeCl_2\cdot4H_2O$), sodium hydroxide (NaOH), acetic acid (CH_3COOH), and methyl orange dye (MO) were of analytical grade and obtained from Aldrich. Beef extract, peptone, and agar powder were of bacteriological grade and *Escherichia coli* (*E. coli*) (KCCM 12119) was used as a model organism to evaluate the antibacterial activity. Deionized water was used throughout the study.

2. Preparation of CS/Fe_3O_4 Composite

In a typical experiment, 0.2 g of Fe_3O_4 nanoparticles prepared by the co-precipitation method [27] was dispersed in 100 mL of 1% (v/v) acetic acid, where Fe_3O_4 was changed to Fe^{3+} and Fe^{2+} cations. To this, 1 g of CS was added and sonicated for 30 min and stirred continuously until a clear solution was obtained. 1 M NaOH was then added dropwise until the solution reached pH 10. The precipitate formed was heated to 80 °C for 5 h and then filtered, washed with an excess of water, and dried overnight in a vacuum oven at 60 °C.

3. Characterization

FT-IR spectroscopy was performed with a Jasco FT/IR-620 spectrometer. The phase and crystallinity were characterized by XRD (Rigaku D/max-2500 X-ray diffractometer) using Cu Kα radiation over the 2θ range, 0-80°. Zeta-potential analysis of the 1 wt% composite dispersed in water was measured by using a Malvern Zetasizer Nano instrument using laser light with a wavelength of 633 nm at 25 °C under a Smoluchowski approximation. The morphology was examined by transmission electron microscopy (TEM, Hitachi H-7600) with an accelerating voltage of 200 kV. The ultraviolet-visible (UV-vis) spectra were recorded with a Jasco V-650 spectrophotometer.

4. Dye Removal Experiment

MO, as an anionic dye (model dye), was used to evaluate the adsorption ability of the composite. The dye removal experiment was conducted at room temperature in batches. In a typical experiment, 100 mg of the MO dye was dissolved in 1 L of distilled water, and the solution pH was varied over the wide range (3-11) by adding phosphate buffer. The required amount of CS/Fe_3O_4 composite was added to the solution and stirred for a predefined time. Then, the composite was separated from the MO solution by a magnetic field. The adsorption amount of MO was estimated from the concentration change of MO in solution after adsorption by UV-vis spectroscopy. The percentage of dye removal was calculated as follows:

$$\text{Percentage of dye removal}=\{(C_0-C_t)/C_0\}\times100 \quad (1)$$

where C_0 is the initial concentration of the dye and C_t is the concentration of the dye at time t. All the experiments were performed in triplicate and the mean value was reported.

5. Antibacterial Activity

E. coli was grown in a nutrient agar (DIFCO 0001) containing 3 g/L beef extract, 5 g/L peptones, and 15 g/L agar in distilled water. The pH of the medium was adjusted to 7.0 by using buffer solution. The antibacterial activity of the CS/Fe_3O_4 composite was evaluated using the colony-forming units (CFU) count method. A freeze-dried sample of the composite was sliced into small pieces and sterilized at 121 °C for 15 min. 9 mL of the growth medium for *E. coli* was added to separate test tubes, and 0.03 g/mL of the finely sliced solid composite samples was added to each of the test tubes. The tubes were then seeded with 1 mL of fresh culture of *E. coli* and incubated at 37 °C for 12 h. The samples were taken after 6, 12, 18, and 24 h for CFU determination. The sample was diluted with saline and cultured on agar plates for 12 h. The CFU was determined by counting the colonies on the agar plates and the mean values were taken from at least three experiments.

RESULTS AND DISCUSSION

Scheme 1 shows the proposed mechanism for the formation of the CS/Fe_3O_4 composite. The process contains two steps. The first step involves the dispersion of CS and Fe_3O_4 nanoparticles in an acetic acid solution, where Fe_3O_4 dissolves and changes into ferric and ferrous ions (Fe^{3+} and Fe^{2+}). The ions immediately form coordination bonds with the -OH and -NH_2 groups of the CS chains [28]. In the second step, the pH of the solution increases to 10 by the dropwise addition of NaOH. A precipitate is formed when the OH^- ions from NaOH coordinate with the Fe^{3+} and Fe^{2+} ions. The precipitate obtained is heated to 80 °C for 5 h to form Fe_3O_4. The homogeneous dispersion of Fe^{3+} and Fe^{2+} in the CS solution aids in the generation of a CS/Fe_3O_4 composite. The proposed reaction of Fe_3O_4 formation in an alkaline solution is as follows.

$$Fe^{2+}+2Fe^{3+}+8OH^-\rightarrow Fe_3O_4+4H_2O$$

Fig. 1 shows the FT-IR spectra of the pure CS and CS/Fe_3O_4 composite. The spectrum of pure CS had a band at 3,370 cm^{-1} due to

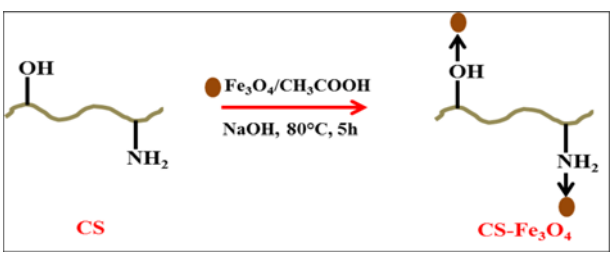

Scheme 1. Schematic representation of the preparation of CS/Fe_3O_4 composite.

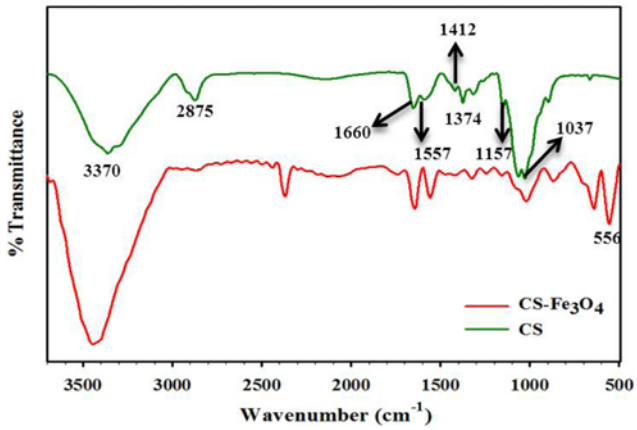

Fig. 1. FT-IR spectra of the CS and CS/Fe_3O_4 composite.

the stretching vibration mode of the -OH and -NH groups. The band at 2,875 cm^{-1} was assigned to the symmetrical stretching of -CH_2 group in the polymer, 1,660 cm^{-1} indicated an amide I group (C-O stretching along the N-H deformation), 1,557 cm^{-1} was attributed to -NH deformation, 1,412 cm^{-1} was assigned to the C-N axial deformation (amine group), 1,374 cm^{-1} was attributed to the COO- group in carboxylic acid salt, 1,157 cm^{-1} was considered the special peak of β (1-4) glucosidic bond in the polysaccharide unit, and 1,037 cm^{-1} was assigned to the stretching vibration of C-O-C in glucose circle [29,30]. The band at 650-1,000 cm^{-1} was attributed to the out-of-plane C-H bending. The band at around 2,400 cm^{-1} was due to CO_2. Compared to CS, a new band at 556 cm^{-1} was observed in the composite due to Fe-O stretching, which confirmed the presence of Fe_3O_4 [31]. In addition, the peaks corresponding to hydroxyl, amino, and amide groups were shifted, indicating the formation of the composite.

Fig. 2 presents the XRD pattern of the CS/Fe_3O_4 composite. The composite shows the XRD patterns of both CS and Fe_3O_4. A small broad peak at 19.8° was assigned to CS [32]. The other diffraction peaks at 30.1°, 35.5°, 43.3°, 53.8°, 57.2°, 63.0°, and 74.8° were assigned to the (220), (311), (400), (422), (511), (440), and (533) planes of Fe_3O_4. The XRD peaks were in good agreement with the cubic Fe_3O_4 [27] showing the successful formation of the CS/Fe_3O_4 composite.

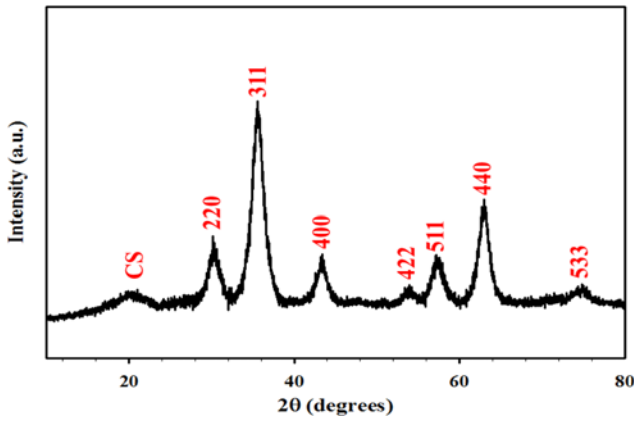

Fig. 2. XRD patterns of the CS and CS/Fe_3O_4 composite.

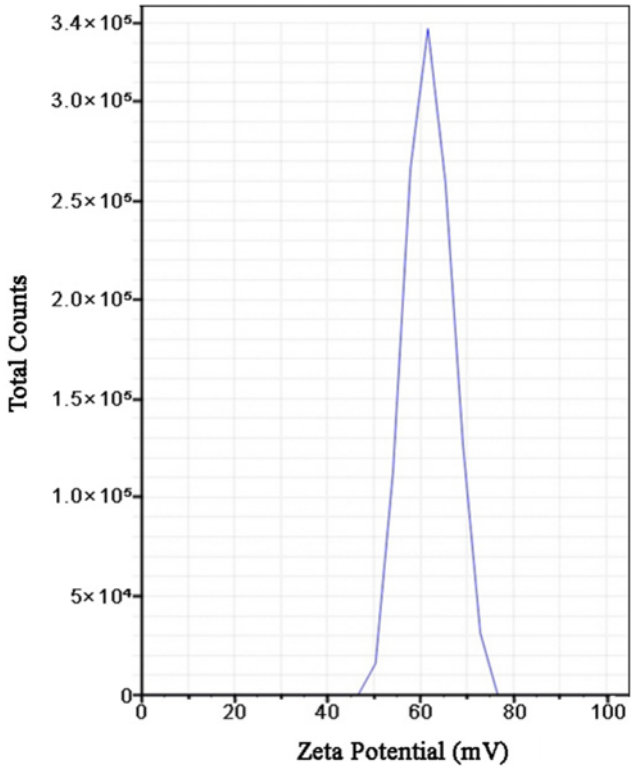

Fig. 3. Zeta potential of the CS/Fe_3O_4 composite at pH 7.

Zeta potential, i.e., surface charge, can greatly influence the particle stability in a suspension through electrostatic repulsion between particles. This property mainly determines the nanoparticle interaction with any species, which is normally negatively charged. Fig. 3 shows the surface of CS/Fe_3O_4 composite has a positive charge about 61.8 mV, while that of Fe_3O_4 has +5.0 mV (which is not shown here). The shift may be attributed to the blockage of active sites on the surface of Fe_3O_4 nanoparticles by adsorbing the polymer chain [32].

TEM provided direct pictorial proof for the immobilization of Fe_3O_4 nanoparticles into CS (Fig. 4). The image shows that Fe_3O_4 nanoparticles coated on the CS surface with an almost uniform distribution. Dark areas in the composite correspond to the crystalline Fe_3O_4 nanoparticles, whereas bright areas represent the amorphous CS. This is due to the high electron density of Fe_3O_4 nanoparticles compared to the CS. The interaction between CS and Fe_3O_4 enhanced the properties of the CS/Fe_3O_4 composite.

Various amounts of CS/Fe_3O_4 composite (0.25-1.0 g/L) were added to 100 mg/L of the dye solution (pH 7) and stirred for 30 min. The composite was separated from the MO solution by a magnet, and the solution was analyzed to determine the dye concentration. Fig. 5 shows the percentage of dye removal. The dye removal reached approximately 95% using 0.5 g of the CS/Fe_3O_4 composite, which was attributed to the larger number of adsorption sites. Further increases in the adsorbent dosage had no effect on the dye removal. Therefore, the optimal dosage for dye removal was 0.5 g of the CS/Fe_3O_4 composite.

The contact time between the adsorbent and adsorbate is one of the most important parameters in the adsorption process. Fig.

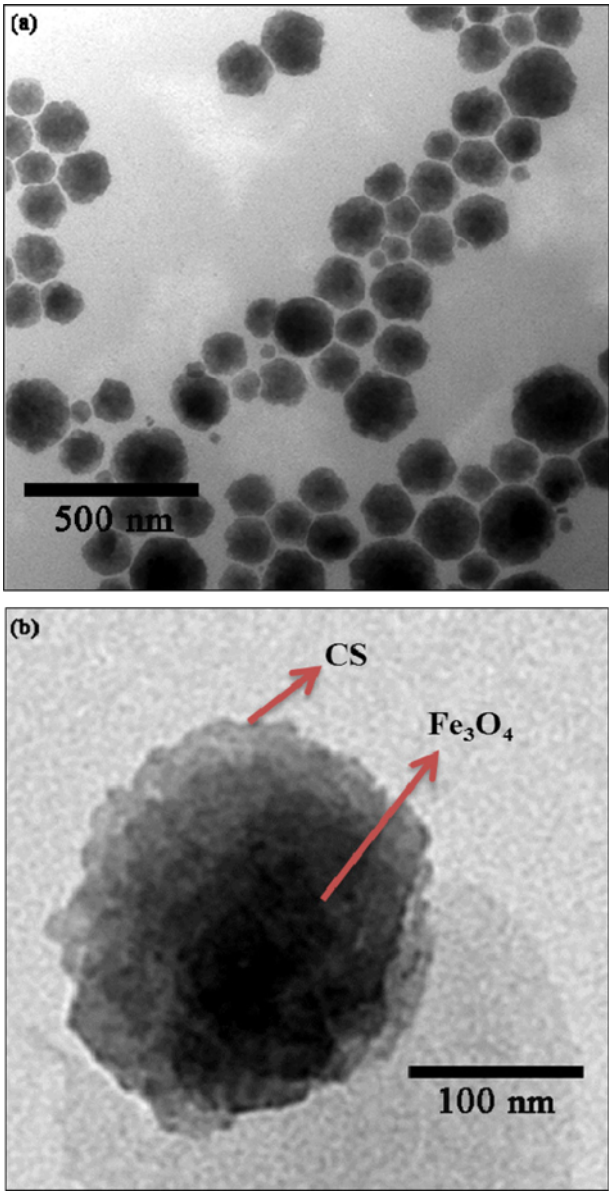

Fig. 4. TEM images of the CS/Fe_3O_4 composite (a) long view and (b) close inspection.

6(a) shows the removal efficiency of the dye by the composite as a function of the stirring time up to 30 min. This shows that adsorption was initiated once the CS/Fe_3O_4 composite added to the dye solution. The removal efficiency reached approximately 95% within 5 min and equilibrium was reached. The optimal time for the dye removal was shorter than the other adsorbents, such as activated carbon and sawdust [33,34]. If an adsorption system has a shorter contact time, the capital and operational costs for real-world applications would be lower, which could be achieved by the CS/Fe_3O_4 composite.

The pH of the solution is another important parameter affecting the adsorption of dye molecules. The effect of solution pH on the dye adsorption was monitored by keeping the dye (100 mg/L) and adsorbent (0.5 g) concentrations constant. The experiments were performed at different pH, ranging from 3 to 11. As shown

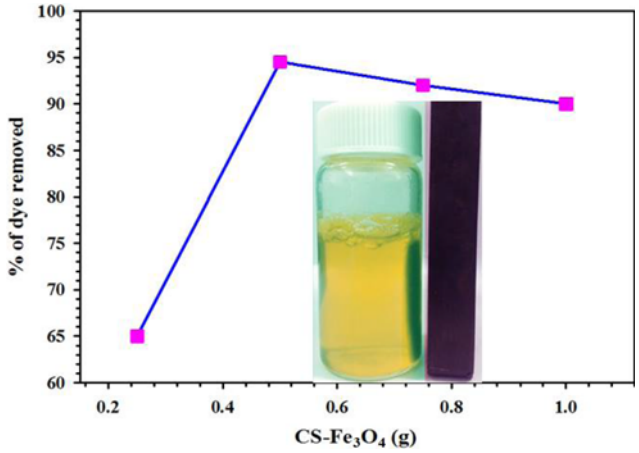

Fig. 5. Effect of adsorbent dosage on the dye adsorption. Inset photograph shows the removal of composite from the dye solution by a magnet.

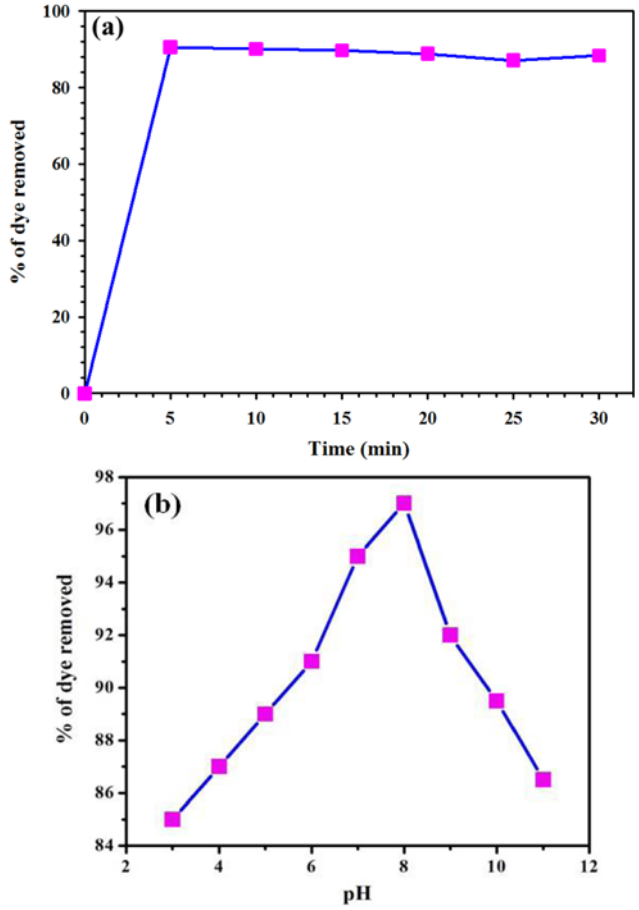

Fig. 6. Effect of (a) stirring time and (b) pH on the dye adsorption.

in Fig. 6(b), the percentage of dye removal increased gradually from 85 to 97% with increasing pH from 3 to 8. This is because the electrostatic interactions between the negatively charged dye molecules and the positively charged CS/Fe_3O_4 composite could be the main adsorption mechanism [35]. On the other hand, a decreasing trend in the efficiency of dye removal was observed with further increas-

ing the pH. This shows that at higher pH (≥8) hydroxyl ions competed with the dye at the adsorption sites on the surface of the CS/Fe_3O_4 composite, leading to a decrease in the percentage of dye removal. The optimal pH was found to be 8.

Dynamic models are of great significance to describe the progress and efficiency of adsorption. Generally, two mathematical models are used, the Lagergren pseudo-first-order equation [36] and pseudo-second-order equation [37], as shown in Eqs. (2) and (3), respectively.

$$\log(q_e - q_t) = \log(q_e) - \left(\frac{k_1}{2.303}\right)t \quad (2)$$

$$\frac{t}{q_t} = \frac{1}{k_2 q_e^2} + \frac{t}{q_e} \quad (3)$$

where k_1 is the rate constant of a pseudo-first-order adsorption (min^{-1}), k_2 is the rate constant of a pseudo-second-order adsorption (g mg^{-1} min^{-1}), t is the adsorption time (min), and q_t and q_e are the adsorption capacity at time t and at equilibrium, respectively (mg g^{-1}).

The experimental data was fitted according to the Lagergren pseudo-first-order equation and pseudo-second-order equation. A good linear plot was obtained for pseudo-second-order reaction model (Fig. 7) with a correlation coefficient R^2 of 0.9997. This suggests that the adsorption rates of the MO dye onto the CS/Fe_3O_4 composite could be described more appropriately using a pseudo-second-order equation. The k_2 and q_e were found to be 0.068 g mg^{-1} min^{-1} and 175.4 mg g^{-1} (87.7%), respectively. The experimental results clearly showed that the CS/Fe_3O_4 composite was an efficient adsorbent for the dye removal from an aqueous solution.

A characteristic feature of an adsorbent from a practical application point of view is its lifetime, because a longer period of time leads to a significant reduction in treatment cost [38]. Therefore, it is essential to evaluate the stability and reuse of the adsorbent for practical implementation. The percentage of dye removal in 5 min was repeated five times using the same adsorbent, and after each experiment, the adsorbent was easily collected for reuse using the magnet. The results indicated that the adsorbent showed a good activity, even after five cycles of reuse (Fig. 8). The slight decrease

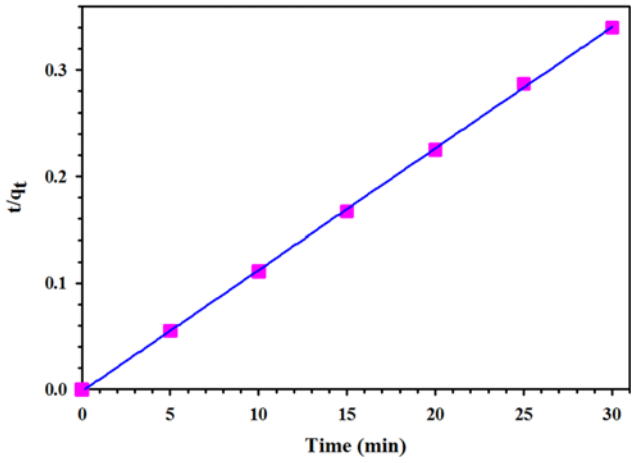

Fig. 7. Pseudo-second-order kinetic plot.

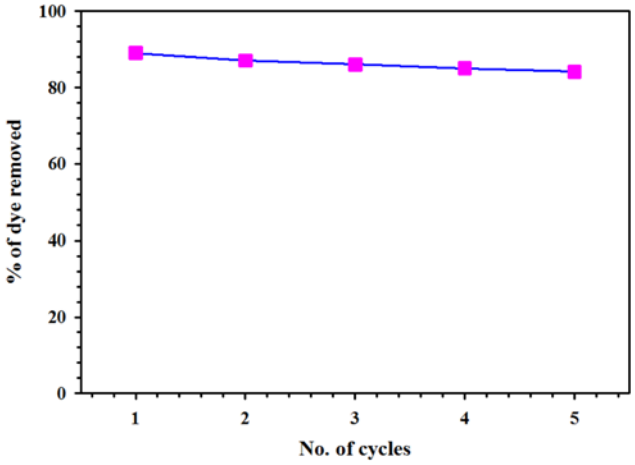

Fig. 8. Efficiency of the CS/Fe_3O_4 composite after five cycles.

Table 1. Antibacterial activity of the CS/Fe_3O_4 composite against *E. coli*

Incubation time (h)	CS		CS/Fe_3O_4 composite	
	CFU (ml^{-1})	Reduction in viability (%)	CFU (ml^{-1})	Reduction in viability (%)
0	28×10^5	0	28×10^5	0
6	6.9×10^5	75.36	71×10^4	68.21
12	1.1×10^6	60.72	45×10^4	73.93
18	1.9×10^6	32.15	31×10^4	76.79
24	2.6×10^6	7.15	18×10^4	81.79

in efficiency might be due to the loss of adsorbent during washing. Nevertheless, the results showed that the CS/Fe_3O_4 composite has a relatively longer shelf life for the dye removal. With respect to clean technology and green chemistry, the low cost, high adsorption efficiency, and excellent reuse, the CS/Fe_3O_4 composite could be an excellent material with the environmentally friendly and sustainable function of self-regeneration.

Table 1 lists the representative results of the viability of *E. coli* after treatment with the CS and CS/Fe_3O_4 composite. The viable bacteria were monitored by counting the number of CFU. The control CS sample inactivated the *E. coli* strain by 7% after 24 h of treatment, showing that almost all the bacteria were alive after 24 h. On the other hand, the CS/Fe_3O_4 composite inactivated the *E. coli* strain by 82% after 24 h. The good reduction in the growth of *E. coli* confirmed the enhanced antibacterial activity of the composite. The antimicrobial activity of the CS was attributed to the interactions with the strongly electronegative microbial surface [39]. The CS-doped Fe_3O_4 showed enhanced antibacterial activity, which was attributed to the effect of both CS and Fe_3O_4 nanoparticles. For reference, we checked the antibacterial activity of Fe_3O_4 nanoparticles and found that the nanoparticles inactivated the *E. coli* strain by around 72% after 24 h. The Gram-negative bacteria have a thin layer of peptidoglycan and a more complex cell wall with two cell membranes. The positively charged CS/Fe_3O_4 composite interacts with the negatively charged lipidic bacterial membrane to alter its permeability, blocking the cells from nutrient intake and ultimately

affecting the cell growth and viability. Biological organisms were killed by the reactive oxygen species generated by Fe_3O_4 nanoparticles [31]. Therefore, this system showed a significantly more efficient bactericidal function for the sterilization of *E. coli*.

CONCLUSIONS

The CS/Fe_3O_4 composite was prepared successfully using a chemical precipitation method. FT-IR and XRD analysis confirmed the formation of the composite. The zeta-potential and TEM analysis confirmed the immobilization of Fe_3O_4 nanoparticles onto the CS. The composite was applied as a novel adsorbent for the removal of MO dye, and the effect of adsorbent dose, pH, and contact time on the removal efficiency of the dye were investigated. The optimal dosage, pH and contact time were 0.5 g, pH 8, and 5 min, respectively. The adsorption kinetics was in good agreement with the pseudo-second-order equation. The results showed that the repeated use of the recycled composite (5 times) did not affect its adsorption efficiency significantly and the adsorbent could be recollected easily using the magnet. Based on the data of the present investigation, the composite being a biocompatible, eco-friendly and low-cost adsorbent is expected to find potential applications in various fields, particularly in environmental applications.

ACKNOWLEDGEMENT

This study was supported by a Yeungnam University research grant in 2012.

REFERENCES

1. G. Moussavi and M. Mahmoudi, *J. Hazard. Mater.*, **168**, 806 (2009).
2. K. Vijayaraghavan and Y.-S. Yun, *Biotechnol. Adv.*, **26**, 266 (2008).
3. F.-C. Wu and R.-L.Tseng, *J. Hazard. Mater.*, **152**, 1256 (2008).
4. M. Zhao, Z. Tang and P. Liu, *J. Hazard. Mater.*, **158**, 43 (2008).
5. H. S. Rai, M. S. Bhattacharyya, J. Singh, T. K. Bansal, P. Vats and U. C. Banerjee, *Crit. Rev. Environ. Sci. Technol.*, **35**, 219 (2005).
6. M. Valix, W. H. Cheung and G. McKay, *Langmuir*, **22**, 4574 (2006).
7. Y. S. Ho and G. McKay, *Chem. Eng. J.*, **70**, 115 (1998).
8. K. Y. Ho, G. McKay and K. L. Yeung. *Langmuir*, **19**, 3019 (2003).
9. P. Liu and L. Zhang, *Sep. Purif. Technol.*, **58**, 32 (2007).
10. E. I. Rabea, M. E.-T. Badawy, C. V. Stevens, G. Smagghe and W. Steurbaut, *Biomacromolecules*, **4**, 1457 (2003).
11. C. M. Yeng, S. Husseinsyah and S. S. Ting, *BioResources*, **8**, 2910 (2013).
12. Z. Liu, H. Bai and D. D. Sun, *New J. Chem.*, **35**, 137 (2011).
13. V. Singh, A. K. Sharma and R. Sanghi, *J. Hazard. Mater.*, **166**, 327 (2009).
14. L. Douziech-Eyrolles, H. Marchais, K. Hervé, E. Munnier, M. Soucé, C. Linassier, P. Dubois and I. Chourpa, *Int. J. Nanomedicine.*, **2**, 541 (2007).
15. G. Reiss and A. Hütten, *Nature Mater.*, **4**, 725 (2005).
16. J. W. M. Bulte and D. L. Kraitchman, *NMR Biomed.*, **17**, 484 (2004).
17. A.-H. Lu, W. Schmidt, N. Matoussevitch, H. Bönnemann, B. Spliethoff, B. Tesche, E. Bill, W. Kiefer and F. Schüth, *Angew. Chem. Int. Edit.*, **43**, 4303 (2004).
18. C. T. Yavuz, J. T. Mayo, W. W Yu, A. Prakash, J. C. Falkner, S. Yean, L. Cong, H. J. Shipley, A. Kan, M. Tomson, D. Natelson and V. L. Colvin, *Science*, **314**, 964 (2006).
19. B. Li, D. Jia, Y. Zhou, Q. Hu and W. Cai, *J. Magn. Magn. Mater.*, **306**, 223 (2006).
20. Y. Wang, B. Li, Y. Zhou and D. Jia, *Polym. Adv. Technol.*, **19**, 1256 (2008).
21. H.-Y. Zhu, Y.-Q. Fu, R. Jiang, J. Yao, L. Xiao and G.-M. Zeng, *Bioresource Technol.*, **105**, 24 (2012).
22. Z. Liu, H. Wang, C. Liu, Y. Jiang, G. Yu, X. Mu and X. Wang, *Chem. Commun.*, **48**, 7350 (2012).
23. G. Dodi, D. Hritcu, G. Lisa and M. I. Popa, *Chem. Eng. J.*, **203**, 130 (2012).
24. C.-Y. Wang, C.-H. Yang, K.-S. Huang, C.-S. Yeh, A. H.-J. Wang and C.-H. Chen, *J. Mater. Chem. B*, **1**, 2205 (2013).
25. G. Huang, H. Zhang, J. X. Shi, T. A. G. Langrish, X. S. Jeffrey and A. G. L. Tim, *Ind. Eng. Chem. Res.*, **48**, 2646 (2009).
26. H. V. Tran, L. D. Tran and T. N. Nguyen, *Mater. Sci. Eng. C*, **30**, 304 (2010).
27. M. Omer, S. Haider and S. y. Park, *Polymer*, **52**, 91 (2011).
28. A. Higazy, M. Hashem, A. ElShafei, N. Shaker and M. A. Hady, *Carbohydr. Polym.*, **79**, 867 (2010).
29. F. Tian, Y. Liu, K. Hu and B. Zhao, *J. Mater. Sci.*, **38**, 4709 (2003).
30. C. M. Yeng, S. Husseinsyah and S. S. Ting, *Polym.-Plast. Technol.*, **52**, 1496 (2013).
31. S. Arokiyaraj, M. Saravanan, N. K. Udaya Prakash, M. Valan Arasu, B. Vijayakumar and S. Vincent, *Mater. Res. Bull.*, **48**, 3323 (2013).
32. Y. Haldorai and J.-J. Shim, *Compos. Interfaces*, **20**, 365 (2013).
33. I. A. W. Tan, A. L. Ahmad and B. H. Hameed, *J. Hazard. Mater.*, **154**, 337 (2008).
34. R. Jain and S. Sikarwar, *J. Hazard. Mater.*, **152**, 942 (2008).
35. Y. S. Al-Degs, M. I. El-Barghouthi, A. H. El-Sheikh and G. M. Walker, *Dyes Pigm.*, **77**, 16 (2007).
36. S. Lagergren, *Kgl. Svenska Vetenskapsakad. Handl.*, **24**, 1 (1898).
37. Y. S. Ho and G. McKay, *Process Biochem.*, **34**, 451 (1999).
38. Y. Haldorai, J.-J. Shim, *Appl. Surf. Sci.*, **292**, 447 (2014).
39. Z. Shariatinia and Z. Nikfar, *Int. J. Biol. Macromol.*, **60**, 226 (2013).